Research Report

BC Journal of Ecosystems and Management

Detecting and mapping mountain pine beetle red-attack damage with SPOT-5 10-m multispectral imagery

Joanne C. White[1], Michael A. Wulder[2], Danny Grills[3]

Abstract

The objective of this study was to gauge the effectiveness of using SPOT-5 10-m multispectral imagery to detect and map red-attack damage for an area near Cranbrook, British Columbia, Canada. A logistic regression model was used to incorporate SPOT imagery with elevation and associated derivatives for red-attack detection and mapping. Separate independent sets of calibration and validation data, collected via a detailed aerial survey, were used to train the classification algorithm and vet the output maps of red-attack damage. The output from the logistic regression model was a continuous surface indicating the probability of red-attack damage. Using a greater than 50% probability threshold, red-attack was mapped with 71% accuracy (with a 95% confidence interval of ±9%). This level of accuracy is comparable to that achieved with Landsat single-date imagery in an area with similar levels of infestation. If a synoptic view of mountain pine beetle red-attack damage at the landscape level is required, and if Landsat data are unavailable, SPOT-5 10-m multispectral imagery may be considered an alternative data source, albeit an expensive one, for detecting and mapping mountain pine beetle red-attack damage.

KEYWORDS: *detection, mountain pine beetle, red-attack, remote sensing, SPOT-5.*

Contact Information

1 Spatial Analyst, Natural Resources Canada, Canadian Forest Service, Pacific Forestry Centre, 506 West Burnside Road, Victoria, BC V8Z 1M5. Email: joanne.white@nrcan.gc.ca

2 Research Scientist, Natural Resources Canada, Canadian Forest Service, Pacific Forestry Centre, 506 West Burnside Road, Victoria, BC V8Z 1M5. Email: mwulder@nrcan.gc.ca

3 Research Associate, Natural Resources Canada, Canadian Forest Service, Pacific Forestry Centre, 506 West Burnside Road, Victoria, BC V8Z 1M5. Email: dgrills@fes.uwaterloo.ca

White, J.C., M.A. Wulder, and D. Grills. 2006. Detecting and mapping mountain pine beetle red-attack damage with SPOT-5 10-m multispectral imagery. *BC Journal of Ecosystems and Management* 7(2)105–118. URL: ***http://www.forrex.org/publications/jem/ISS35/vol7_no2_art11.pdf***

Introduction

The mountain pine beetle (*Dendroctonus ponderosae* Hopkins) is the most destructive insect of mature pine forests in western North America (Wood 1963). In British Columbia, the mountain pine beetle infestation increased from 164 000 ha in 1999 to 8.7 million ha in 2005 (British Columbia Ministry of Forests and Range 2006). The two main factors that have contributed to the successful expansion of the beetle population in British Columbia include the large amount of mature lodgepole pine (*Pinus contorta* Dougl. ex Loud. var. *latifolia* Engelm.) on the land base, which has tripled in the last century as a result of intensive fire suppression activities (Taylor and Carroll 2004), and several successive years of favourable climatic conditions, which has resulted in an increase in suitable areas for brood development (Carroll *et al.* 2004).

In general, mountain pine beetles in British Columbia reproduce at a rate of one generation per year (Safranyik *et al.* 1974). Adult beetles typically attack trees in August, and lay eggs that develop into mature adults approximately 1 year later. The beetles must attack in large numbers to overcome the defences of a healthy tree. Once killed, but still with green foliage, the host tree is in the green-attack stage. The foliage of the host tree changes colour gradually. Twelve months after attack, over 90% of the killed trees will have red needles (red-attack). Three years after attack, most trees will have lost all needles (grey-attack) (B.C. Ministry of Forests 1995). Generally, the foliage fades from green to yellow to red over the spring and summer following attack (Amman 1982; Henigman *et al.*1999).

From a forest management perspective, estimates of the location and extent of mountain pine beetle red-attack are critical; however, the degree of precision required for these estimates varies according to the management objective under consideration and the nature of the mountain pine beetle infestation. The range of information requirements is matched by a hierarchy of different data sources that are currently used to map red-attack damage, with each data source offering a different level of detail on location and extent.

Vegetation and land cover have been mapped using SPOT-4 20-m and SPOT-5 10-m multispectral satellite data (e.g., Gong and Howarth 1992; Jacquin *et al.* 2005). Several studies have compared the performance of Landsat Thematic Mapper (TM) and Enhanced Thematic Mapper (ETM+) to that of SPOT-4 and SPOT-5 data for vegetation applications (e.g., Franklin *et al.* 1994; May *et al.* 1997; Gao 1999; Harvey and Hill 2001; Darvishsefat *et al.* 2004). These studies (with the exception of Franklin *et al.* [1994] and Darvishsefat *et al.* [2004]), found that the greater spectral resolution of Landsat data resulted in improved discrimination of vegetation types over that of the SPOT data. Thus, despite its greater spatial resolution, SPOT data was generally outperformed by Landsat data. Franklin *et al.* (1994) found no statistically significant differences between the results produced with Landsat or SPOT data. Darvishsefat *et al.* (2004) compared the performance of SPOT-5 5-m and 10-m data to Landsat 7 ETM+ data for forest mapping, and concluded that the SPOT-5 10-m data were more suitable than Landsat for forest mapping at a scale of 1:25 000.

The mountain pine beetle is the most destructive insect of mature pine forests in western North America.

Forest damage, such as defoliation (Franklin 1989; Brockhaus *et al.* 1992) and catastrophic events (Schwarz *et al.* 2001; Lin *et al.* 2004), has been mapped using SPOT data. Sirois and Ahern (1988) used SPOT 20-m multispectral data to map red-attack damage caused by mountain pine beetle; red-attack damage was detected through visual interpretation and manual digitizing. Using this method, damage locations had to be at least 1–2 ha, with 80–100% of the trees at the location having red-attack damage (Sirois and Ahern 1988), before the damage could be detected visually on the SPOT image.

The objective of our study was to explore the potential of single-date SPOT multispectral imagery to detect and map mountain pine beetle red-attack damage in an area with relatively low infestation levels using an automated classification procedure. In doing so, issues unique to SPOT, and the potential offered by the higher spatial resolution of SPOT compared with Landsat, could be identified. The viability of SPOT as an alternative data source to Landsat could then be assessed.

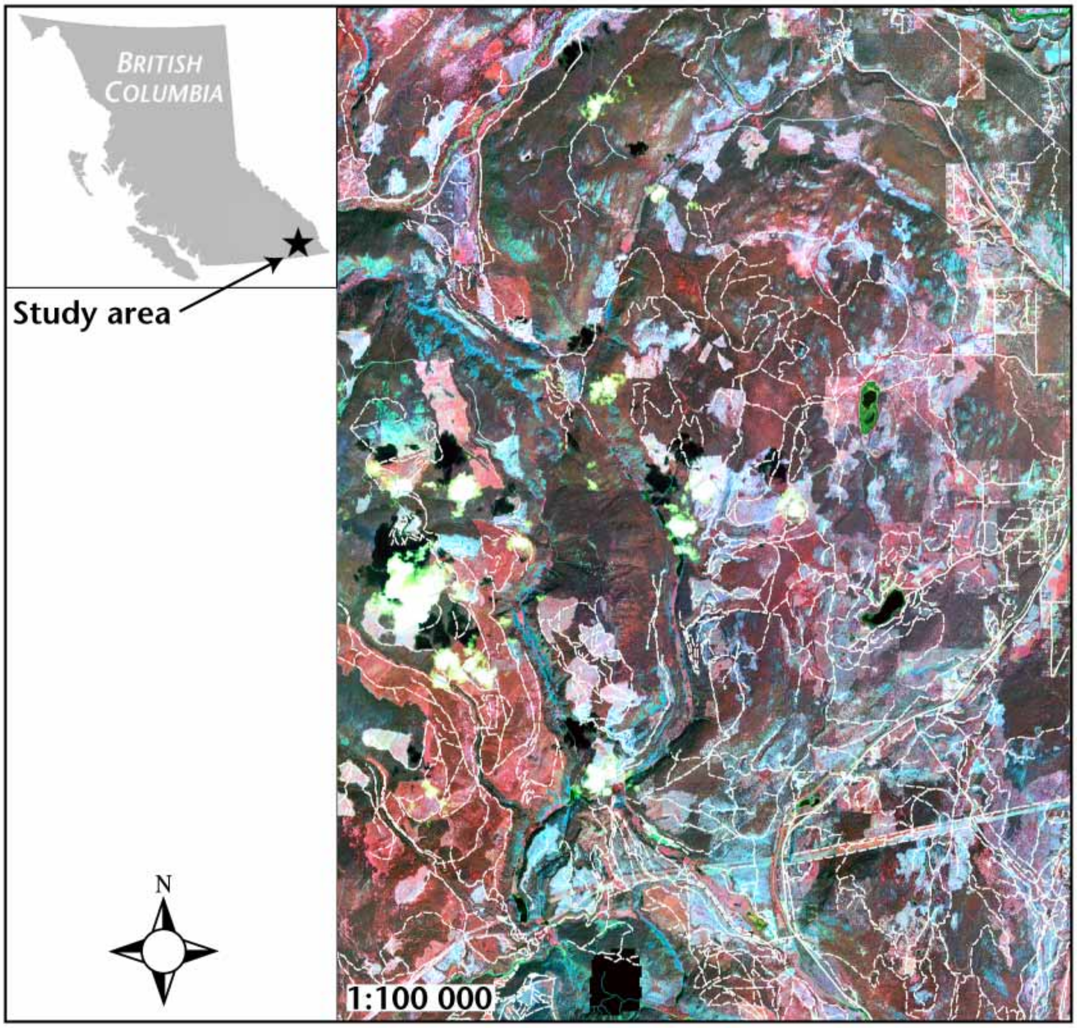

FIGURE 1. Study area location near Cranbrook, B.C.

Study Area

The study area covers approximately 32 000 ha and is located 30 km west of Cranbrook, B.C. (Figure 1). The biogeoclimatic zones found in this area include Montane Spruce (MS), Interior Douglas-fir (IDF), Engelmann Spruce–Subalpine Fir (ESSF), Ponderosa Pine (PP), and Interior Cedar–Hemlock (ICH). The MS is the largest zone, representing 46% of the study area, followed closely by the IDF, which represents 42% of the study area. The MS biogeoclimatic zone lies between the high-elevation subalpine forests and the lower-elevation forests of the IDF. The climate is dry. Average temperatures extend above 10°C for 2–4 months and stay below 0°C for nearly 5 months of the year. Lodgepole pine generally dominates this zone, but the attributes of nearby biogeoclimatic zones greatly affect the species composition. The climate in the IDF tends to be dry year round with moderate temperatures generally found at lower elevations. The IDF is populated mainly by Douglas-fir (*Pseudotsuga menziesii* [Mirbel] Franco *var. menziesii*), but also has large lodgepole pine populations at higher elevations. The elevation in the study area ranges from 818 m to 2295 m, with a mean elevation of 1222 m.

The forest species found in the study area include lodgepole pine, western larch (*Larix occidentalis* Nutt.), and Douglas-fir, with smaller amounts of Engelmann spruce (*Picea engelmannii* Parry), yellow pine (*Pinus ponderosa* Laws.), alpine fir (*Abies lasiocarpa* [Hook] Nutt.), balsam poplar (*Populus balsamifera* L.),

TABLE 1. A summary of leading forest species in the study area and associated attributes

Species	Area (ha)	Total volume (m^3)	DBH (cm)[a,b]	Crown closure (%)[b]	Age (years)[b]	Height (m)[b]	Stems per hectare[b]
Balsam poplar/ cottonwood	44	77 698	34.10	43.27	130	31.49	No data
Aspen	42	52 050	21.49	58.37	69	22.81	1180
Alpine fir	180	32 345	14.21	38.89	107	19.37	752
Douglas-fir	4499	1 034 195	21.02	36.68	130	20.17	428
Alpine larch	7	523	5.82	42.00	140	16.34	0
Western larch	6482	1 548 812	19.48	46.88	126	23.64	294
Whitebark pine	36	19 286	24.44	52.03	195	21.10	0
Lodgepole pine	6660	2 307 183	15.92	44.97	70	16.84	1171
Yellow pine	416	135 419	18.82	25.45	126	23.82	21
Engelmann spruce	447	390 625	24.28	41.60	126	24.94	615

[a] Diameter at breast height.
[b] Average values.

cottonwood (*Populus trichocarpa* [Torr. and Gray]), aspen (*Populus tremuloides* Michx.), whitebark pine (*Pinus albicaulis* Engelm.), and alpine larch (*Larix lyalii* Parl.) (Table 1). Lodgepole pine covers approximately 35% of the forested land in the study area and constitutes 41% of the total volume.

Forest harvesting activities have altered much of the landscape and cutblocks cover approximately 36% of the study area. Many of the cutblocks are less than 7 years old and frequently occur among lodgepole pine stands. Table 2 provides a summary of infestation severity and area, as estimated by annual aerial overview surveys. Between 1999 and 2003, the area affected by the mountain pine beetle fluctuated between 500 and 800 ha. In 2004, the area of damage increased markedly, to approximately 2000 ha (Figure 2); however, this is a relatively low level of damage, representing only 7% of the total study area, or approximately 10% of the total area covered by lodgepole pine.

TABLE 2. Area of mountain pine beetle red-attack damage estimated from annual aerial overview survey data collected for the study site between 1999 and 2004

Year	Area (ha)
1999	832
2000	427
2001	No data
2002	863
2003	543
2004	2220

Data

SPOT Data

On July 22, 2004, SPOT-5 10-m (Level 1A) multispectral data were acquired, with approximately 13% of the image area covered in cloud (Figure 1). The sun elevation was 59.0° and the sun azimuth was 154.1°. The view angle was close to nadir at –1.7°. The multispectral images were acquired in three bands (green: 0.50–0.59 mm; red: 0.61–0.68 mm; near infrared (NIR): 0.78–0.89 mm) at a 10-m spatial resolution, combined with a shortwave infrared band (SWIR) (1.58–1.75 mm) acquired at 20 m. The SWIR band was resampled to 10 m to generate the final four-band image. The image was orthorectified, using available planimetric and elevation data, with a root mean square error of less than one pixel.

Mountain Pine Beetle Survey Data

To facilitate detailed detection and mapping of red-attack, 1:30 000 conventional colour aerial photography was acquired by the B.C. Ministry of Forests in 2004. Photos were collected during the appropriate

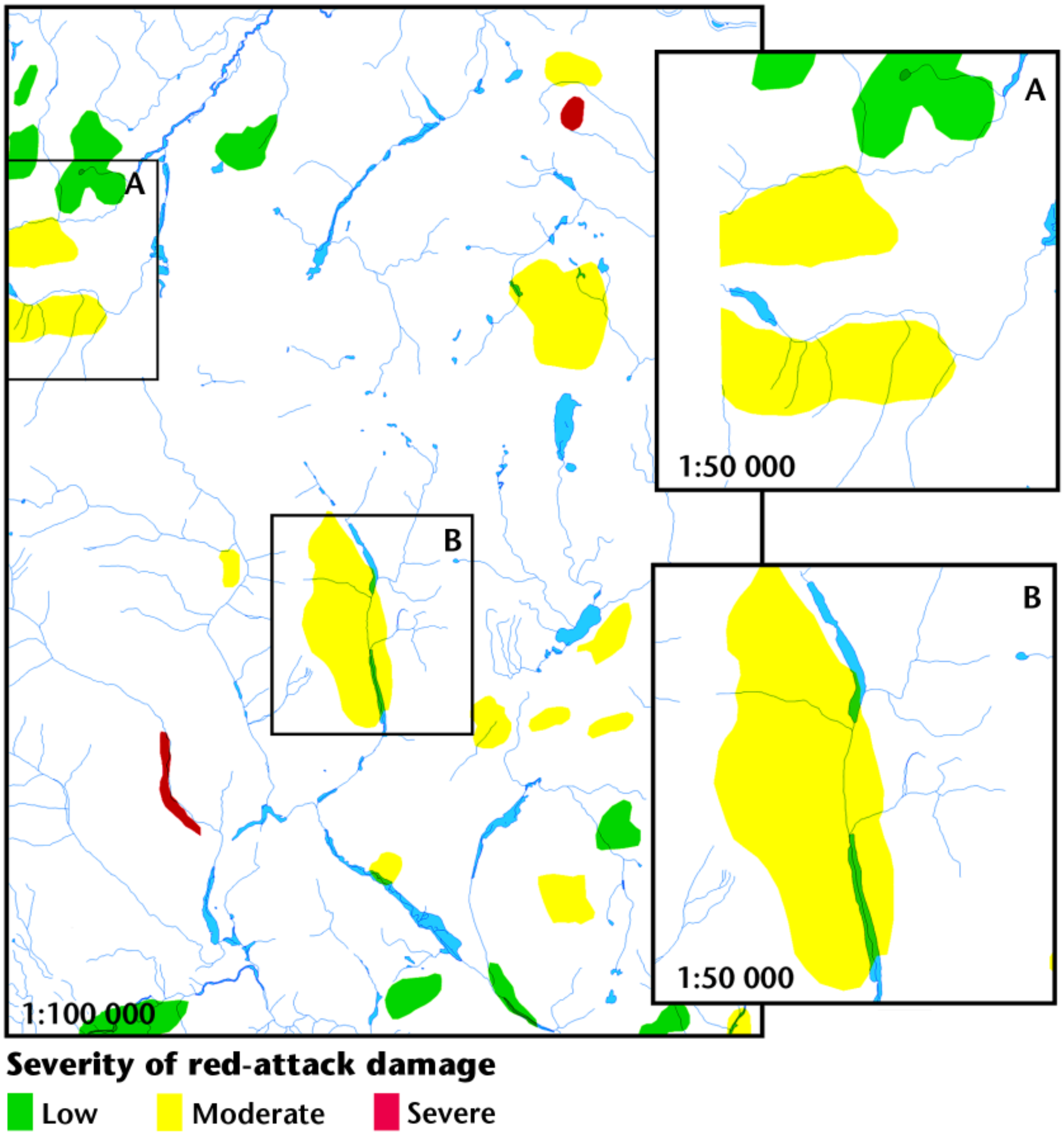

FIGURE 2. Mountain pine beetle damage as captured by aerial overview surveys in the summer of 2004.

bio-window between July and mid-September (Wulder *et al.* 2005) in those areas that had been identified for suppression in the province's strategic beetle management plan (B.C. Ministry of Forests 2003). The air photos were then digitized (scanned) at a high resolution (maximum of 14 mm) (Nelson *et al.* 2000). Red-attack damage was visually interpreted from the photos using digital photogrammetric software, and an output map of red-attack areas was generated. The photos provide a permanent record of the survey, and may be used for other purposes such as the update of topographic base maps. The red-attack maps are a hybrid product composed both of polygons (depicting broad areas of red-attack) and points (providing a specific location and number of red-attack trees), depending on the spatial extent of the damage at a particular location. Red-attack maps were acquired for two B.C. Geographic Map Series (BCGS) 1:20 000 mapsheets: 82G041 and 82G051 (Figure 3). Table 3 contains a summary of the polygon data. Note that data scale and differing collection methods resulted in dissimilar estimates of red-attack damage area; that is, a 914-ha estimate from the red-attack map data compared to a 2220-ha estimate for the aerial overview survey data. The mapped point locations were subsequently used as calibration and validation for red-attack damage.

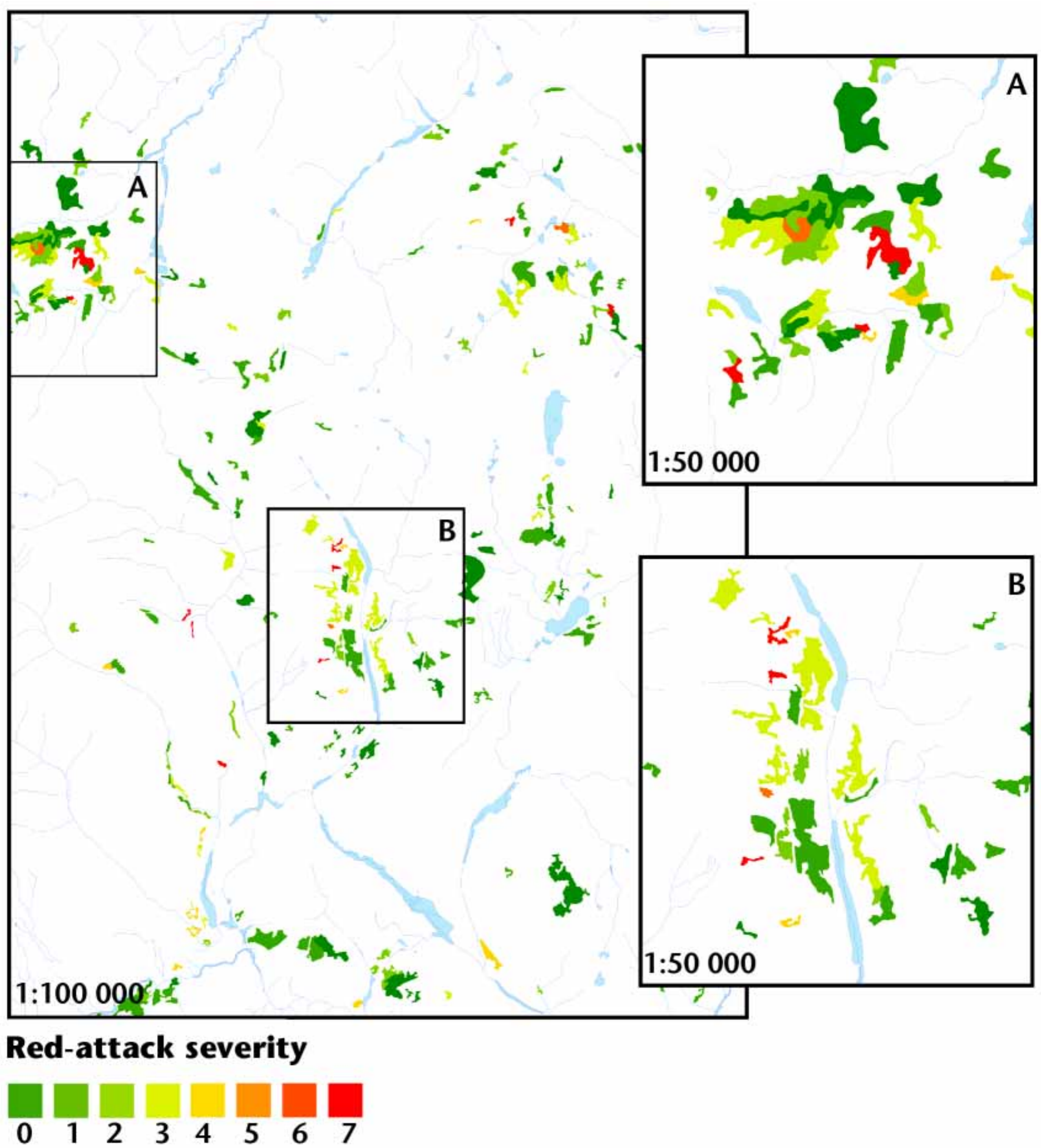

FIGURE 3. Photo-interpreted estimates of red-attack damage in the study area. Areas in red indicate red-attack damage interpreted from 1:30 000 photography acquired in the summer of 2004.

TABLE 3. Area of mountain pine beetle red-attack damage estimated from aerial photography (interpreted from 1:30 000 colour air photos) collected in 2004 using more detailed severity ratings

% Severity	Area (ha)	% Severity	Area (ha)
0.1–10	269	51–60	10
11–20	308	61–70	14
21–30	123	71–80	8
31–40	146	81–90	0
41–50	36	91–100	0
Total			*914*

Forest Inventory

The data were collected between 1964 and 1998, with all attributes projected to 2000. Each of the forest polygons contains a large number of attributes including:

- area (m^2),
- crown cover,
- diameter at breast height (DBH),
- age,
- height (m),
- stems per hectare, and
- volume (m^3).

A pine mask was generated to restrict subsequent image analysis procedures (Franklin *et al.* 2003). The forest inventory was queried and forest stands that contained greater than 40% pine (by volume) and that had an average stand age of greater than 60 years were included in the pine mask.

Digital Elevation Model

In addition to the remotely sensed imagery, a digital elevation model (DEM) with a 25-m spatial resolution was available for the study area (B.C. Ministry of Sustainable Resource Management 2002). Slope was estimated within a window of 3 × 3 cells using the average maximum technique (Burrough 1986; Oksanen and Sarjakoski 2005).

Solar Radiation

Solar radiation and related variables can aid in the prediction of vegetation type and growth (Franklin 1995). Direct clear-sky solar radiation was calculated using the equation developed by Kreith and Kreider (1978) and implemented using a process developed by Kumar *et al.* (1997). Direct solar radiation is the radiation received directly on a horizontal surface, without any absorption or scattering. Diffuse solar radiation is the portion of the solar radiation that is scattered downwards by the molecules in the atmosphere. Diffuse solar radiation varies between summer and winter, and is a function of solar altitude and terrain reflectance. Global solar radiation is calculated by summing direct and diffuse solar radiation. Wulder *et al.* (2006b) tested the use of diffuse, direct, and global solar radiation in a logistic regression model for detection of red-attack damage. None of the predictor variables were found to be significant in the study area, which was located in the Lolo National Forest in Montana (Wulder *et al.* 2006b).

Methods

In this study, mountain pine beetle red-attack damage was detected and mapped using a logistic regression approach, with a forward stepwise selection process and a set of calibration data representing samples of red-attack and non-attack from the study area. The variables considered for inclusion in the model were the four SPOT-5 10-m spectral channels, elevation, slope, and solar radiation (direct, diffuse, and global). The discrete nature of the dependent variable (i.e., red-attack, non-attack) was well suited to the use of logistic regression. Logistic regression has become a widely used and accepted method of analysis of binary outcome variables, as it is flexible and predicts the probability for the state of a dichotomous variable based on predictor variables. Details regarding the logistic regression approach followed in this study can be found in Wulder *et al.* (2006b).

Selection of Calibration and Validation Data

The red-attack points identified from aerial photography were used to locate suitable training pixels for red-attack damage. The points were stratified using a forest structure mask (Franklin *et al.* 2003). The photo-interpreted map points and polygons, which identified locations of known red-attack damage, were overlaid with the pine mask. Pine stands in the mask that were not spatially coincident with the air photo mapping data were considered to represent non-attack conditions. Calibration points for red-attack and non-attack were further refined by eliminating points that had other associated damage agents, or which had grey-attack damage. Four equal-sized samples were selected for red-attack and non-attack calibration and validation data from the available sample points remaining ($n = 115$).

Model Validation

Model validation was performed by calculating fit statistics and prediction errors. The Hosmer and Lemeshow's Goodness of Fit measure tests the null hypothesis that the data were generated by the model fitted by the researcher (Hosmer and Lemeshow 2000). If the p value is greater than 0.05, the model's estimates fit the data at an acceptable level at 95% of probability. The Wald statistic was used to test the null hypothesis in logistic regression that a single coefficient was zero, verifying the significance of individual logistic regression coefficients for each independent variable (Norusis 2005). In addition, the adjusted logistic model was applied to generate an output map of red-attack damage, which was subsequently validated using the reserved independent validation dataset. The error matrix for the binary variable (predicted vs. observed) was generated, omission and commission errors were determined, and associated 95% confidence intervals calculated (Czaplewski 2003). The overall accuracy and true positive rate were also calculated. The true positive rate is the attribute-specific accuracy for red-attack; this measure reports how many red-attack trees identified from the image source were actually identified as red-attack in the validation data (e.g., producer's accuracy).

Results

Table 4 presents the parameters of the logistic regression model along with measures of model performance. The Hosmer and Lemeshow Goodness of Fit Test indicates the model estimates fit the data within an acceptable level ($\alpha = 0.05$). The Wald statistic indicates that the red and NIR bands, direct solar radiation, and elevation were significant to the model. Table 4 also provides the odds ratio, e^{β}, and the percentage change in the odds ratio. Per-unit changes in reflectance in the red band or in direct solar radiation resulted in an increase of 4% and 0.01%, respectively, in the odds of red-attack damage. Conversely, increases in NIR reflectance or in elevation resulted in a decrease in the odds of red-attack damage by 11.6% and 0.3%, respectively.

Figure 4 depicts the continuous probability surface, which indicates the likelihood of red-attack damage. For validation purposes, a threshold value of 50% was used to discriminate between red-attack and non-attack. Therefore, if a pixel had a probability of red-attack of less than or equal to 50%, the pixel was considered as non-attack. Conversely, if the pixel had a probability of greater than 50%, the pixel was considered red-attack. Table 5 presents a confusion matrix that contains the results of the accuracy assessment. The overall accuracy of the logistic regression model was estimated at 64% (95% confidence interval ±6%). The true positive rate (producer's accuracy) for red-attack damage was estimated at 71% (95% confidence interval ±9%).

Discussion and Summary

Most jurisdictions use aerial overview surveys to detect red-attack damage at the landscape level (Wulder *et al.* 2006a) and more detailed surveys are then undertaken as required (Wulder *et al.* 2006b). Multiple dates of Landsat TM and ETM+ have been used to successfully detect and map red-attack damage at the landscape scale with accuracies of 81% (95% confidence interval ±11%) in areas where the damage occurs in fairly large, contiguous patches (30–50 red-attack trees) (Skakun *et al.*

TABLE 4. Parameters of the logistic regression model, developed using forward stepwise selection. All of the SPOT image bands were included as input into the model, as were elevation, slope, and direct, diffuse and global solar radiation. The SPOT red and NIR bands, elevation, and direct solar radiation were included in the final model.

		Wald Test		Hosmer and Lemeshow
Model parameters	α_i	**Wald**	**Significance**	**Goodness of Fit Test**
Intercept	9.872	22.761	0.000	
Red	0.038 $e^{\beta} = 1.038$ change in odds ≈ 4%	6.687	0.010	**Chi-square** 8.045
NIR	–0.123 $e^{\beta} = 0.884$ change in odds ≈ –11.6%	17.482	0.000	**Significance** 0.429
Direct	0.001 $e^{\beta} = 1.001$ change in odds ≈ 0.01%	4.009	0.045	
Elevation	–0.003 $e^{\beta} = 0.997$ change in odds ≈ –0.3%	17.128	0.000	

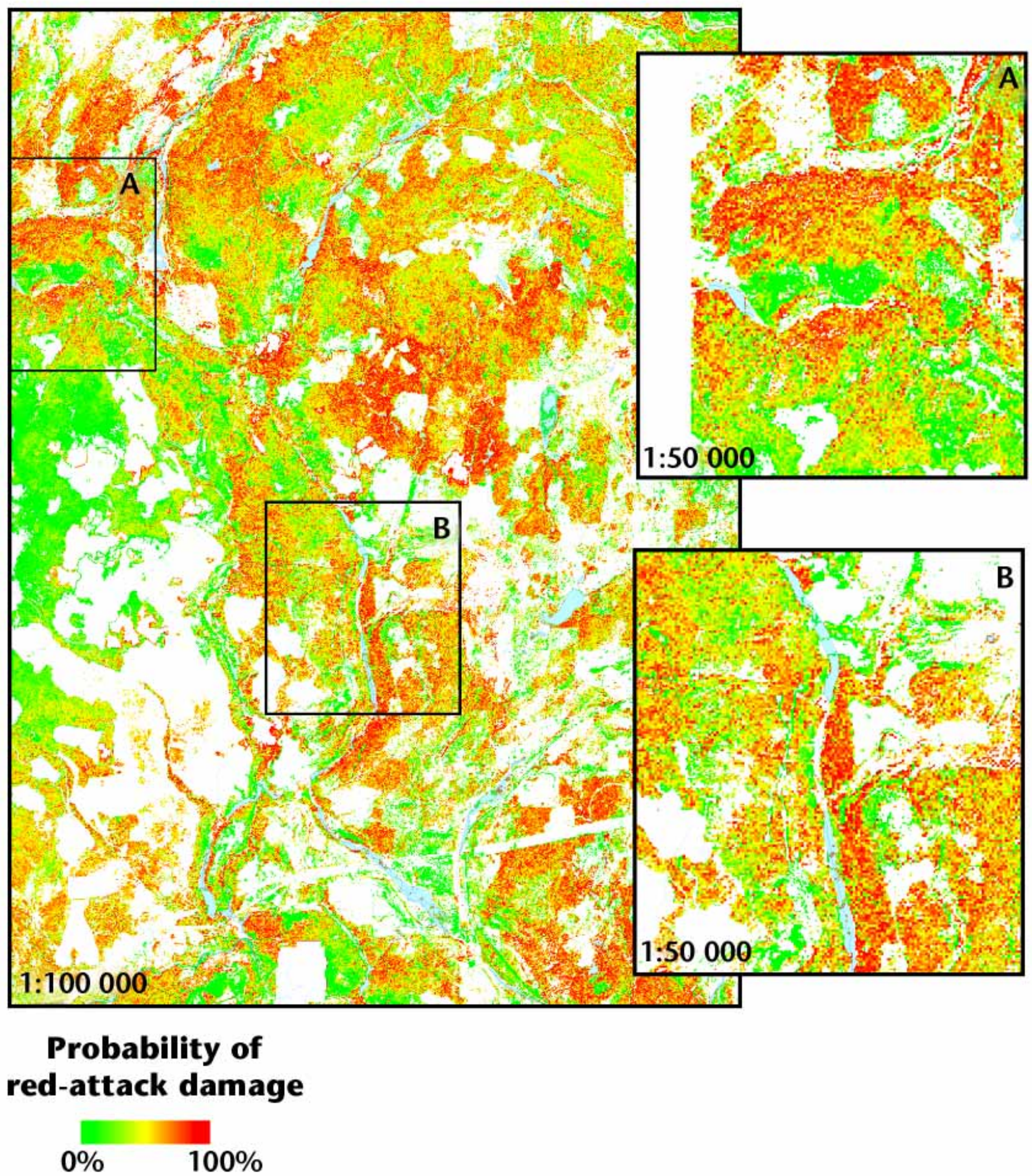

FIGURE 4. Probability of mountain pine beetle red-attack damage as output from a logistic regression model generated using SPOT image bands (red and NIR), direct solar radiation, and elevation.

2003). Single-date Landsat imagery has also been used to map red-attack damage with an accuracy of 73% (95% confidence interval ±10%) (Franklin *et al*. 2003). High-resolution IKONOS imagery has been used to map damage in stands in which less than 5% of the trees are red-attack, with an accuracy of 70% (95% confidence interval ±8%), and stands in which 5–20% of trees are red-attack, with an accuracy of 93% (95% confidence interval ±2%) (White *et al*. 2005). QuickBird data has also been used to map red-attack damage in individual stands for areas in which the level of infestation was considered low to moderate (Coops *et al*. 2006).

To provide information on the area and proportion of each stand that contained red-attack damage, the estimates derived from the SPOT data were integrated into the existing forest inventory using polygon decomposition (Wulder and Franklin 2001; Wulder *et al*. 2005). Table 6 provides a comparison of red-attack damage

TABLE 5. Confusion matrix containing the results of the accuracy assessment

<table>
<tr><th colspan="2" rowspan="2">Predictors:
SPOT-RED, SPOT-NIR, DIRECT SOLAR RADIATION, AND ELEVATION</th><th colspan="3">Logistic model</th><th rowspan="2">Producer's accuracy</th><th colspan="2" rowspan="2">Omission error</th></tr>
<tr><th>Non-attack</th><th>Red-attack</th><th>Total</th></tr>
<tr><td rowspan="3">Reference data</td><td>Non-attack</td><td>64</td><td>51</td><td>115</td><td>56%</td><td colspan="2">44%</td></tr>
<tr><td>Red-attack</td><td>33</td><td>82</td><td>115</td><td>71%</td><td colspan="2">28%</td></tr>
<tr><td>Total</td><td>97</td><td>133</td><td>230</td><td colspan="3">Overall accuracy</td></tr>
<tr><td colspan="2">User's accuracy</td><td>66%</td><td>62%</td><td rowspan="2"></td><td>Lower CI</td><td>Value</td><td>Upper CI</td></tr>
<tr><td colspan="2">Comission error</td><td>34%</td><td>38%</td><td>58%</td><td>64%</td><td>70%</td></tr>
</table>

TABLE 6. Estimates of red-attack damage from the aerial overview survey, air photo interpretation, and logistic regression with SPOT data for 2004 decomposed to the forest inventory polygon level

Percent of	Aerial overview survey	Photo interpreted	SPOT
Total stands	14	18	39
Total stand area	7	3	5
Forested stands	16	21	45
Total forested area	8	3	6
Pine stands	21	27	59
Total pine area	10	4	7

from the different information sources. Using a threshold probability value of greater than 50% to identify red-attack damage, 39% of the forest inventory polygons showed such damage, accounting for 5% of the total study area and 7% of the total area of pine. In contrast, the aerial overview survey, which is collected at a coarser spatial scale (Wulder *et al.* 2006b), identified 14% of forest inventory polygons as having red-attack damage, representing 7% of the total study area, or 10% of the total pine area. Estimates of red-attack damage provided by photo interpretation indicated levels of damage between those of the SPOT data and the aerial overview survey. The scale and methods of data collection, as well as the nature of the infestation, contribute to the discrepancies in damage estimates in Table 6 (Wulder *et al.* 2005). Figures 2, 3, and 4 illustrate the differences and the similarities between the spatial depictions of damage for each of these data sources.

This study demonstrates that SPOT data can provide an alternative to Landsat data for the detection and mapping of mountain pine beetle damage at the landscape level. Landsat-5 has experienced technical difficulties in the past, and a scan-line corrector problem on Landsat-7 has necessitated the production of mosaicked image products. The status of the Landsat program is therefore somewhat unpredictable and the exploration of alternative data sources is ongoing (Williamson and Baker 2004). The SPOT sensor has a different set of spectral bands than the Landsat (Table 7), and some research indicates that Landsat outperforms SPOT for vegetation applications, despite the greater spatial resolution of the SPOT imagery. As mountain pine beetle damage results in moisture loss (Reid 1961; Yamaoka *et al.* 1990), and the SWIR portion of the spectrum is sensitive to water content in vegetation (Ceccato *et al.* 2001), the absence of a second band in the SWIR region of the electromagnetic spectrum may affect the detection of red-attack damage with SPOT-5 10-m multispectral imagery. Note that the SPOT-5 SWIR band is collected at 20-m resolution and resampled to 10 m.

Our results should be considered in the context of similar studies that have used single-date remotely sensed data to detect and map red-attack damage.

TABLE 7. Comparison of spectral properties, spatial resolution, and relative costs of remotely sensed data sources used for red-attack detection and mapping. Cost assumes archive imagery is available. SPOT and IKONOS instruments do not collect data continuously, so additional acquisition costs would apply if no archive imagery was available for the study area.

Band	Landsat	SPOT-5	IKONOS
Blue	0.45–0.52		0.45–0.52
Green	0.52–0.60	0.50–0.59	0.52–0.60
Red	0.63–0.69	0.61–0.68	0.63–0.69
NIR	0.76–0.90	0.78–0.89	0.76–0.90
MIR	1.55–1.75	1.58–1.75	
MIR	2.08–2.35		
Spatial resolution	30 m	10 m	4 m
Cost for study area (CAD$, 308 km^2)	$6.16	$1232.00	$2802.00
Reported accuracies for red-attack detection (true positive rate)	Franklin *et al.* (2003) 73% (95% CI ±10%)	Results of this study 71% (95% CI ±9%)	White *et al.* (2005) **< 5% damage:** 70% (95% CI ±8%) **5–20% damage:** 93% (95% CI ±2%)

For example, Franklin *et al.* (2003) used single-date Landsat TM imagery to detect red-attack damage in an area that had infestation levels (in 1999) similar to those of the Cranbrook study site in 2004. The scenes produced with SPOT-5 10-m imagery have a smaller image footprint than those produced with Landsat TM or ETM+ data (3600 km^2 vs. 31 000 km^2). Logistically, this means that multiple SPOT-5 scenes are required to cover the same area as a single Landsat scene, which results in increased data handling issues and processing costs. Furthermore, the use of multiple SPOT-5 scenes requires some form of radiometric normalization and (or) image mosaicking before classification.

Table 7 indicates the relative cost of acquiring Landsat TM, SPOT, or IKONOS data for the Cranbrook study area. Although SPOT data can provide accuracy comparable to that of Landsat, the cost difference between SPOT and Landsat is large. The logistical issues associated with mapping larger areas of damage, as mentioned previously, further contribute to mapping costs. To justify the increased cost of using SPOT-5 10-m data in an operational context, the end-user should expect significant gains in accuracy over what is achievable with Landsat data. If higher accuracies for red-attack detection are required in areas with very low infestation levels, then either IKONOS or QuickBird data, both of which are significantly more expensive than Landsat or SPOT, would be appropriate choices (White *et al.* 2005). Both IKONOS and QuickBird data have small image footprints, however, and therefore all of the previously mentioned logistical issues would be applicable to these data sources as well. Our study results demonstrate that if landscape-level maps of red-attack damage are required, and Landsat TM or ETM+ data are not available, SPOT-5 10-m data could be considered as an alternative data source. If available, however, a time series of Landsat imagery does offer improved landscape-level detection of red-attack damage (Skakun *et al.* 2003; Wulder *et al.* 2006b). A multi-date approach using SPOT-5 10-m data could possibly result in similar improvements in red-attack detection accuracy.

Our study results demonstrate that if landscape-level maps of red-attack damage are required, and Landsat TM or ETM+ data are not available, SPOT-5 10-m data could be considered as an alternative data source.

Acknowledgements

David Seemann of the Canadian Forest Service, and Flor Alvarez of the Universidad de León, are thanked for assistance with image processing and analysis. This study is part of an ongoing project funded by the Government of Canada through the Mountain Pine Beetle Initiative, a 6-year, $40 million program administered by Natural Resources Canada, Canadian Forest Service. Additional information on the Government of Canada supported Mountain Pine Beetle Initiative may be found at: *http://mpb.cfs.nrcan.gc.ca/about_e.html*

References

Amman, G.D. 1982. The mountain pine beetle: Identification, biology, causes of outbreaks, and entomological research needs. *In* Proceedings of the joint Canada/USA workshop on mountain pine beetle related problems in western North America. D.M. Shrimpton (editor). Environment Canada, Canadian Forestry Service, Pacific Forest Research Centre, Victoria, B.C. Information Report BC-X-230. pp. 7–12.

British Columbia Ministry of Forests. 1995. Bark beetle management guidebook. Forest Practices Code of British Columbia, Victoria, B.C. URL: *http://www.for.gov.bc.ca/tasb/legsregs/fpc/fpcguide/beetle/betletoc.htm*

________. 2003. Timber supply and the mountain pine beetle infestation in British Columbia. Forest Analysis Branch, Victoria, B.C. URL: *http://www.for.gov.bc.ca/hts/pubs/beetledoc_oct29LO.pdf*

B.C. Ministry of Forests and Range. 2006. Mountain pine beetle affects 8.7 million hectares. Press Release: March, 2006. Victoria, B.C. URL: *http://www.for.gov.bc.ca/hfp/mountain_pine_beetle/2005MPBsurvey.pdf*

B.C. Ministry of Sustainable Resource Management. 2002. Gridded digital elevation model product specifications. Edition 2.0. Base Mapping and Geomatics Services Branch, Victoria, B.C.

Brockhaus, J., S. Khorram, R. Bruck, M. Campbell, and C. Stallings. 1992. A comparison of Landsat TM and SPOT HRV data for use in the development of forest defoliation models. International Journal of Remote Sensing 13:3235–3240.

Burrough, P.A. 1986. Principles of geographical information systems for land resources assessment. Clarendon Press, Oxford, U.K.

Carroll, A.L., S.W. Taylor, J. Régnière, and L. Safranyik. 2004. Effects of climate change on range expansion by the mountain pine beetle in British Columbia. *In* Mountain pine beetle symposium: Challenges and solutions, October 30–31, 2003, Kelowna, B.C. T.L. Shore, J.E. Brooks, and J.E. Stone (editors). Natural Resources Canada, Canadian Forest Service, Pacific Forestry Centre, Victoria, B.C. Information Report BC-X-399. pp. 223–232.

Ceccato, P., S. Flasse, S. Tarantola, S. Jacquermoud, and J.M. Gregoire. 2001. Detecting vegetation leaf water content using reflectance in the optical domain. Remote Sensing of Environment 77:22–33.

Coops, N.C., M. Johnson, M.A. Wulder, and J.C. White. 2006. Assessment of QuickBird high spatial resolution imagery to detect red attack damage due to mountain pine beetle infestation. Remote Sensing of Environment 103:67–80.

Czaplewski, R.L. 2003. Accuracy assessment of maps of forest condition. *In* Remote sensing of forest environments: Concepts and case studies. M.A. Wulder and S.E. Franklin (editors). Kluwer Academic Publishers, Boston, Mass. pp. 115–140.

Darvishsefat, A.A., P. Fatehi, A.K. Pour, and A. Farzaneh. 2004. Comparison of SPOT-5 and Landsat-7 for forest area mapping. *In* Geo-imagery bridging continents. Proceedings of the 20th ISPRS Congress, Commission 7, July 12–23, 2004, Istanbul, Turkey. International Society for Photogrammetry and Remote Sensing, London, U.K. URL: *http://www.isprs.org/istanbul2004/comm7/papers/82.pdf*

Franklin, J. 1995. Predictive vegetation mapping: Geographic modelling of biospatial patterns in relation to environmental gradients. Progress in Physical Geography 19:474–499.

Franklin, S.E. 1989. Classification of hemlock looper defoliation using SPOT HRV imagery. Canadian Journal of Remote Sensing 15:178–182.

Franklin, S.E., D.R. Connery, and J.A. Williams. 1994. Classification of alpine vegetation using Landsat Thematic Mapper, SPOT HRV, and DEM data. Canadian Journal of Remote Sensing 20:49–56.

Franklin, S.E., M.A. Wulder, R. Skakun, and A. Carroll. 2003. Mountain pine beetle red attack damage classification using stratified Landsat TM data in British Columbia, Canada. Photogrammetric Engineering and Remote Sensing 69:283–288.

Gao, J. 1999. A comparative study on spatial and spectral resolutions of satellite data in mapping mangrove forests. International Journal of Remote Sensing 20:2823–2833.

Gong, P. and P.J. Howarth. 1992. Land-use classification of SPOT HRV data using a cover-frequency method. International Journal of Remote Sensing 13:1459–1471.

Harvey, K.R. and G.J.E. Hill. 2001. Vegetation mapping of a tropical freshwater swamp in the Northern Terrotory, Australia: A comparison of aerial photography, Landsat TM and SPOT satellite. International Journal of Remote Sensing 22:2911–2925.

Henigman, J., T. Ebata, E. Allen, and A. Pollard. (editors). 1999. Field guide to forest damage in British Columbia. B.C. Ministry of Forests, Victoria, B.C.

Hosmer, D.W. and S. Lemeshow. 2000. Applied logistic regression. Wiley-Interscience, New York, N.Y.

Jacquin, A., V. Cheret, J.P. Deneux, M. Gay, J. Mitchley, and P. Xofis. 2005. Habitat suitability modelling of capercaillie (*Tetrao urogallus*) using earth observation data. Journal for Nature Conservation 13:161–169.

Kreith, F. and J.F. Kreider. 1978. Principles of solar engineering. McGraw-Hill, New York, N.Y.

Kumar, L., A.K. Skidmore, and E. Knowles. 1997. Modelling topographic variation in solar radiation in a GIS environment. International Journal for Geographical Information Science 11:475–497.

Lin, C.Y., H.M. Lo, W.C. Chou, and W.T. Lin. 2004. Vegetation recovery assessment at the Jou-Jou Mountain landslide area caused by the 921 earthquake in central Taiwan. Ecological Modelling 176:75–81.

May, A.M.B., J.E. Pinder, and G.C. Kroh. 1997. A comparison of Landsat Thematic Mapper and SPOT multispectral imagery for the classification of shrub and meadow vegetation in northern California, U.S.A. International Journal of Remote Sensing 18:3719–3728.

Nelson, T., M.A. Wulder, and K.O. Niemann. 2000. Spatial resolution implications of digitizing aerial photography for environmental applications. Imaging Science Journal 49:223–232.

Norusis, M.J. 2005. SPSS 13.0 Advanced statistical procedures. Prentice Hall, N.J.

Oksanen, J. and T. Sarjakoski. 2005. Error propagation of DEM-based surface derivatives. Computers and Geosciences 31:1015–1027.

Reid, R.W. 1961. Moisture changes in lodgepole pine before and after attack by the mountain pine beetle. Forestry Chronicle 37:368–375.

Safranyik, L., D.M. Shrimpton, and H.S. Whitney. 1974. Management of lodgepole pine to reduce losses from the mountain pine beetle. Department of the Environment, Canadian Forest Service, Pacific Forest Research Centre, Victoria, B.C. Forestry Technical Report No. 1.

Schwarz, M., C. Steinmeier, and L. Waser. 2001. Detection of storm losses in alpine forest areas by different methodic approaches using high-resolution satellite data. eCognition Application Note, Volume 2.

Sirois, J. and F.J. Ahern. 1988. An investigation of SPOT HRV data for detecting mountain pine beetle mortality. Canadian Journal of Remote Sensing 14:104–108.

Skakun, R.S., M.A. Wulder, and S.E. Franklin. 2003. Sensitivity of the Thematic Mapper Enhanced Wetness Difference Index (EWDI) to detect mountain pine needle red attack damage. Remote Sensing of Environment 86:433–443.

Taylor, S.W. and A.L. Carroll. 2004. Disturbance, forest age, and mountain pine beetle outbreak dynamics in B.C.: A historical perspective. *In* Mountain pine beetle symposium: Challenges and solutions, October 30–31, 2003, Kelowna, B.C. T.L. Shore, J.E. Brooks, and J.E. Stone (editors). Natural Resources Canada, Canadian Forest Service, Pacific Forestry Centre, Victoria, B.C. Information Report BC-X-399. pp. 41–51.

White, J.C., M.A. Wulder, D. Brooks, R. Reich, and R. Wheate. 2005. Detection of red attack stage mountain pine beetle infestation with high spatial resolution satellite imagery. Remote Sensing of Environment 96:340–351.

Williamson, R.A. and J.C. Baker. 2004. Current US remote sensing policies: Opportunities and challenges. Space Policy 20:109–116.

Wood, S.L. 1963. A revision of bark beetle genus *Dendroctonus erichson* (Coleoptera: Scolytidae). Great Basin Naturalist 23:1–117.

Wulder, M.A. and S.E. Franklin. 2001. Polygon decomposition with remotely sensed data: Rationale, methods, and applications. Geomatica 55:11–21.

Wulder, M.A., R.S. Skakun, S.E. Franklin, and J.C. White. 2005. Enhancing forest inventories with mountain pine beetle infestation information. Forestry Chronicle 81:149–159.

Wulder, M.A., C.C. Dymond, J.C. White, D.G. Leckie, and A.L. Carroll. 2006a. Surveying mountain pine beetle damage of forests: A review of remote sensing opportunities. Forest Ecology and Management 221:27–41.

Wulder, M.A., J.C. White, B. Bentz, F.A. Alvarez, and N.C. Coops. 2006b. Estimating the probability of mountain pine beetle red-attack damage. Remote Sensing of Environment 101:150–166.

Yamaoka, Y., R.H. Swanson, and Y. Hiratsuka. 1990. Inoculation of lodgepole pine with four blue-stain fungi associated with mountain pine beetle, monitored by a heat pulse velocity (HPV) instrument. Canadian Journal of Forest Research 20:31–36.

ARTICLE RECEIVED: **April 3, 2006**
ARTICLE ACCEPTED: **August 2, 2006**

Test Your Knowledge . . .

Detecting and mapping mountain pine beetle red-attack damage with SPOT-5 10-m multispectral imagery

How well can you recall some of the main messages in the preceding research report? Test your knowledge by answering the following questions. Answers are at the bottom of the page.

1. Which of the following is not a potential host for mountain pine beetle?
   A) Lodgepole pine
   B) Whitebark pine
   C) Douglas-fir
   D) Ponderosa pine

2. The attack stage most readily detected and mapped with remotely sensed data is:
   A) Grey-attack
   B) Adult stage
   C) Red-attack
   D) Green-attack

3. True positive accuracy represents:
   A) The average number of red-attack trees that were correctly classified.
   B) The number of red-attack trees identified from the model output that were identified as red-attack by the validation data.
   C) The number of non-attacked trees identified from the model output that were identified as non-attacked by the validation data.
   D) The number of red-attack trees identified from the model output that were not identified as red-attack by the validation data.

ANSWERS

1. C 2. C 3. B